doi:10.1111/evo.13788

Cross-sex genetic covariances limit the evolvability of wing-shape within and among species of *Drosophila*

Jacqueline L. Sztepanacz[1,2] and David Houle[1]

[1]*Department of Biology, Florida State University, Tallahassee, Florida 32306*

[2]*E-mail: jsztepanacz@gmail.com*

Received February 14, 2019

Accepted May 29, 2019

The independent evolution of males and females is potentially constrained by both sexes inheriting the same alleles from their parents. This genetic constraint can limit the evolvability of complex traits; however, there are few studies of multivariate evolution that incorporate cross-sex genetic covariances in their predictions. *Drosophila* wing-shape has emerged as a model high-dimensional phenotype; wing-shape is highly evolvable in contemporary populations, and yet perplexingly stable across phylogenetic timescales. Here, we show that cross-sex covariances in *Drosophila melanogaster*, given by the B-matrix, may considerably bias wing-shape evolution. Using random skewers, we show that B would constrain the response to antagonistic selection by 90%, on average, but would double the response to concordant selection. Both cross-sex within-trait and cross-sex cross-trait covariances determined the predicted response to antagonistic selection, but only cross-sex within-trait covariances facilitated the predicted response to concordant selection. Similar patterns were observed in the direction of extant sexual dimorphism in *D. melanogaster*, and in directions of most and least dimorphic variation across the *Drosophila* phylogeny. Our results highlight the importance of considering between-sex genetic covariances when making predictions about evolution on both macro- and microevolutionary timescales, and may provide one more explanatory piece in the puzzle of stasis.

KEY WORDS: **B-matrix, constraint, evolvability, G-matrix, sexual dimorphism, stasis.**

The evolvability of a population is determined by the amount of genetic variation in the traits that are targets of selection. Genetic variation has been found for almost every individual trait (Barton and Partridge 2000; Blows and Hoffmann 2005; Walsh and Lynch 2018). However, much of this variation may not be useful to selection because of linkage disequilibrium, in the short term, or pleiotropy in the long term. Pleiotropy produces covariation among traits, orienting new genetic variation that arises from mutation (Houle and Fierst 2013; McGuigan et al. 2015; Hine et al. 2018), and standing genetic variation (Walsh and Blows 2009), into a smaller number of multivariate trait combinations. This may leave other multivariate trait combinations with little genetic variation (Kirkpatrick 2008; Gomulkiewicz and Houle 2009). Since Lande (1979) proposed the multivariate breeder's equation, the role of genetic variances and covariances, summarized in the **G** matrix, in shaping the response to selection has been widely explored (e.g., Blows and Hoffmann 2005; Hansen and Houle 2008; Walsh and Blows 2009). Using this framework, we can predict which multivariate trait combinations are constrained because of limited genetic variation. Constraints will most often lead to multivariate selection responses that are stochastic (Hine et al. 2014), slow, or biased toward directions of most genetic variation (Schluter 1996; Chenoweth et al. 2010). In contrast, when selection targets those trait combinations with high levels of genetic variation, the response to selection in a particular trait may be augmented beyond that expected from a univariate model (Agrawal and Stinchcombe 2009).

Most studies of constraint have considered the role of **G** without regard to sex. However, both selection and genetic variation can differ between the sexes, resulting in more complex effects of **G** during adaptation. In many cases, selection will be sexually antagonistic, favoring different equilibrium phenotypes in males

and females. Therefore, we also need to consider the covariances between traits expressed in different sexes as potential sources of constraint. The divergence of sexually homologous traits seems particularly likely to be constrained because of the shared alleles that underlie them. This may make it difficult for one or both sexes to achieve their fitness optima, resulting in intralocus sexual conflict (Bonduriansky and Chenoweth 2009; Cox and Calsbeek 2009). Theory predicts that sexual conflict is a frequent byproduct of adaptation in species with separate sexes, regardless of the form of selection on each sex (Connallon and Clark 2013). When selection favors a different optimal trait value in each sex, and there is insufficient genetic variation to allow each sex to reach its optimum, mutations with similar phenotypic effects will tend to improve the fitness of one sex, while hurting the other. Conversely, when selection is sexually concordant and mutations have dissimilar effects on the two sexes it will be difficult to achieve similar phenotypes, again creating antagonism in the effects on fitness. More complex scenarios are also possible where there is no permanent equilibrium level of dimorphism or conflict, suggesting that the role of **G** will be important for both transient and equilibrium sexual antagonism (Pennell et al. 2016).

There are many examples of intralocus sexual conflict, for example, over locomotor activity in *Drosophila* (Long and Rice 2007), diet in crickets (Maklakov et al. 2008), and fitness itself (Foerster et al. 2007; Collet et al. 2016; Wolak et al. 2018). However, the occurrence of sexual dimorphism in many species suggests that intralocus sexual conflict can sometimes be resolved. The empirical work on this topic has focused on the role of intersexual genetic correlations for single traits. There are relatively few studies that quantify constraints imposed by multivariate cross-sex covariances (Steven et al. 2007; Barker et al. 2010; Campbell et al 2010; Lewis et al. 2011; Gosden et al. 2012; Reddiex et al 2013; Gosden and Chenoweth 2014; Ingleby et al. 2014; Walling et al. 2014; Cox et al. 2017), despite the fact that bivariate correlations rarely reflect the larger multivariate patterns of covariance (Conner and Via 1993; Blows and Hoffmann 2005; Hansen and Houle 2008; Walsh and Blows 2009).

Lande (1980) proposed a generalization of the multivariate breeder's equation to include differences in selection and inheritance in the two sexes. The equation,

$$\begin{bmatrix} \Delta\bar{z}_m \\ \Delta\bar{z}_f \end{bmatrix} = \frac{1}{2} \begin{bmatrix} \mathbf{G}_m & \mathbf{B}' \\ \mathbf{B} & \mathbf{G}_f \end{bmatrix} \begin{bmatrix} \beta_m \\ \beta_f \end{bmatrix}$$

predicts the responses in males ($\Delta\bar{z}_m$) and females ($\Delta\bar{z}_f$). Similarly, the selection gradient includes a vector for both males (β_m) and females (β_f). The expanded **G** matrix, $\mathbf{G}_{mf}$, includes the symmetric within-sex (co)variances among traits for males and females ($\mathbf{G}_m$ and $\mathbf{G}_f$), and **B**, the covariances of homologous traits expressed in both males and females. The diagonal elements of **B** quantify the amount of genetic variation that is shared between the sexes for the same trait, whereas the off-diagonal elements quantify cross-sex cross-trait covariances. Unlike $\mathbf{G}_m$ and $\mathbf{G}_f$, **B** is not necessarily symmetric. This reflects the fact that alleles can differ in the amount of variation that they cause when expressed in males versus in females (Gosden and Chenoweth 2014). All three submatrices of $\mathbf{G}_{mf}$ affect the response to selection. Here, we focus on the effect of **B**, which we can decompose into three parts. First, biased selection responses could arise due to the shared genetic variance between males and females for the same trait, represented by the diagonal elements of **B**. Second, the response may also be affected by the off-diagonal elements of **B**, the covariances between different traits, *i* and *j*, expressed in different sexes. We can partition the off-diagonal of **B** into a symmetric component, representing the shared cross-sex, cross-trait covariances that do not depend on which sex expresses trait *i* or *j*, and an asymmetric component representing the differences in covariance when trait *i* is expressed in a male and *j* in a female, versus when trait *i* is expressed in a female and *j* in a male.

Until recently, most studies have applied Lande's (1980) approach to a single trait, and have focused on the standardized intersexual genetic correlation $\boldsymbol{r}_{mf,}$ to infer the degree to which sexual dimorphism can evolve (Lynch and Walsh 1998; Poissant et al. 2009; Delph et al. 2011). Indeed, Poissant et al. (2009) reviewed 488 estimates of $\boldsymbol{r}_{mf}$ from 114 studies, all of which were focused on a single trait. Half of the estimates were above 0.8, suggesting that the evolution of sexual dimorphism may often be constrained. Consistent with this, Poissant et al. (2009) found a negative relationship between $\boldsymbol{r}_{mf}$ and the degree of sexual dimorphism; traits with large positive intersexual correlations were less dimorphic while traits with small correlations showed a wide range of dimorphism. Therefore, the evolution of sexual dimorphism may often be constrained by high intersexual correlations. Inferences from studies of $\boldsymbol{r}_{mf}$, however, are limited for at least three reasons. First, studies have tended to focus on sexually dimorphic traits that are generally expected to experience sexually antagonistic selection. For example, of the 395 studies with estimates of sexual dimorphism that Poissant et al (2009) reviewed, 67% of traits were dimorphic by 10% or more. Second, one cannot say from an $\boldsymbol{r}_{mf}$ value and an estimate of sexual dimorphism whether there is ongoing sexual conflict. Third, as highlighted earlier, a single-trait approach overlooks multivariate genetic covariances between traits that are expressed in both sexes, which are fundamental for predicting responses to multivariate selection (Wyman et al. 2013).

A growing number of studies have incorporated multivariate cross-sex covariances in evolutionary predictions, utilizing Lande's (1980) extension of the multivariate breeder's equation. These studies have tended to focus on visibly dimorphic (Lewis et al. 2011; Gosden et al. 2012; Ingleby et al. 2014; Cox et al. 2017) and sexually selected traits (Gosden et al. 2012; Ingleby

et al. 2014; Cox et al. 2017). In almost every case, **B** potentially limits the response to antagonistic selection by biasing both the magnitude (Lewis et al. 2011; Ingleby et al. 2014; Cox et al. 2017) and direction (Lewis et al. 2011; Gosden et al. 2012) of the predicted response to estimated selection vectors or to random selection vectors. The role of **B** in biasing predicted evolutionary responses in traits that are not known or expected to experience sexually antagonistic selection has been quantified by only two studies. Cox et al. (2017) showed that **B** had little effect on the predicted response to selection in random directions, and Holman and Jacomb (2017) showed that **B** facilitated the response to sexually concordant selection. Therefore, **B** may have an equally important role in facilitating the response to selection. Indeed, an analysis of 424 selection gradient estimates by Cox and Calsbeek (2009) found that selection was sexually concordant in 59–83% of the estimates, and a formal meta-analysis of these data similarly found that 75–88% of the estimates were sexually concordant (Morrissey 2016). If we focus only on visibly dimorphic and sexually selected traits, we may be missing the larger effect of **B** on evolutionary trajectories for most traits in most populations.

In some studies, **B** appears to affect the response in females more than it does in males (Lewis et al. 2011; Gosden et al. 2012; White et al. 2018), which may be a consequence of stronger directional selection acting on male traits and stronger stabilizing selection on female traits (Wyman and Rowe 2014). Sex-specific responses can also differ when selection acts in the same way between the sexes, as a consequence of asymmetry in **B**, $\mathbf{G}_m$ or $\mathbf{G}_f$. Asymmetry is a common feature of **B** (Steven et al. 2007; Barker et al. 2010; Lewis et al. 2011; Gosden and Chenoweth 2014; Walling et al. 2014; Ingleby et al. 2014); however, only one study has directly quantified the proportion of covariance that is asymmetric, finding a range from 10 to 40 % depending on the population studied (Gosden and Chenoweth 2014). No one has attempted to quantify how much of the predicted bias in evolutionary responses that are caused by **B** is due to the three components of **B**: the diagonal elements and both the symmetric and asymmetric components of the off-diagonal elements.

Here, we estimate **B** and characterize its evolutionary consequences for a high-dimensional set of sexually homologous wing-shape traits of *D. melanogaster*. Wing shape in *Drosophila* has become a model system for the study of high-dimensional phenotypes (Houle et al. 2003, 2010), and genetic constraints. Several analyses have demonstrated the presence of genetic variation in all multivariate combinations of wing-shape traits for males and females separately (Mezey and Houle 2005; Houle and Meyer 2015; Sztepanacz and Blows 2015), suggesting that wing shape may be evolvable in all directions. Selection experiments in the lab support this, with rapid evolution often observed in response to artificial selection on wing-shape (e.g., Weber 1990; Pélabon et al. 2010; Bolstad et al. 2015). Despite the correlative and manipulative evidence for high evolvability of wing-shape in contemporary populations, wing-shape is remarkably stable across the *Drosophila* phylogeny (Houle et al. 2017). Compared to many other insect species *Drosophila* wings are not very sexually dimorphic (Gidaszewski et al. 2009). We do not know whether the relative lack of dimorphism and the remarkable evolutionary stasis that we observe in *Drosophila* wings are due to selection or due to multivariate genetic constraints. In an experiment where evolution was only allowed to proceed through males, individual wing-shape traits in *D. melanogaster* evolved to be more male like and in the direction of extant sexual dimorphism. Males in the evolved populations experienced a fitness benefit while females experienced a cost, providing evidence for intralocus sexual conflict (Abbott et al. 2010).

To address these unanswered questions, we use our estimate of **B** to characterize how multivariate, cross-sex covariances affect the evolvability of a population of *D. melanogaster* across the entire phenotypic space and in the direction of extant sexual dimorphism. We also identify how **B** constrains the divergence in sexual dimorphism among 75 species of *Drosophila*. Specifically, we quantify how the three components of **B** constrain or facilitate the predicted responses to multivariate selection.

Methods

EXPERIMENTAL DESIGN

The analyses presented here were performed on a previously published data set; the detailed methods of the experiment can be found in Mezey and Houle (2005). Briefly, using a laboratory population initiated from 140 isofemale lines, a series of half-sibling breeding experiments were carried out over 36 temporally replicated blocks with an average of five sires per block. Each sire was mated to four or five virgin dams, and dams were allowed to oviposit individually for 2 days in each of two replicate vials. Upon eclosion, approximately five males and five females from each replicate oviposition vial were collected. One wing from each parent and each offspring were imaged using an automated image analysis system (Houle et al. 2003) and the *x*- and *y*-coordinates of 12 vein intersections (Fig. 1 in Mezey and Houle 2005) were recorded. The data were aligned by generalized Procrustes least squares superimposition, resulting in an estimate of wing size, and size-adjusted *x*- and *y*-coordinates that describe the relative displacement of each landmark from the centroid. One degree of freedom is lost to estimate wing size and three degrees of freedom are lost to standardize the orientation of wing shapes. Therefore, there are a maximum of 20 variable dimensions in the aligned *x*-, *y*-coordinate data. These coordinates capture variation in wing shape in units of centroid

size. In total, the breeding design consisted of 175 sires, 803 dams, and 17,325 individuals of which there were approximately equal numbers of males and females. Multivariate outliers of the 24 *x*-*y*-coordinates were identified using Mahalanobis distance, and a total of 124 multivariate outliers (0.7% of the data set) were removed prior to analyses. The phenotypic covariance matrix (**P**) of the 24 *x*-*y*-coordinates was calculated as $\mathbf{P} = \frac{\mathbf{XX}'}{n-1}$, and phenotypic scores on the first 20 principal components of **P** that have variation (Table S1) were used as traits in all subsequent analyses.

SEXUAL DIMORPHISM

The major axis of sexual dimorphism can be described by the multivariate trait combination that differs the most in mean between males and females. To determine this trait combination, we performed a linear discriminant analysis of the 20 principal components of wing-shape with sex as the discriminant variable, using the lda function in the MASS package in R. The discriminant function is the multivariate trait combination (vector) that maximizes the separation between male and female wing shapes. We obtained the error in the estimate of this multivariate trait combination by bootstrapping the data at the level of sire 500 times, and re-estimating the discriminant function for each sample of the data. To visualize how this vector relates to the difference in wing shape between males and females, we used the program Lory (Marquez et al. 2012). We show the relative pattern of contraction and expansion in the original 12 *x*- and *y*-coordinates of the average female wing, compared to the average male wing. To determine whether there was genetic variation in the direction of sexual dimorphism, and consequently the opportunity for flies to evolve in this multivariate trait combination, we fit a linear mixed effects animal model with a single response variable using restricted maximum likelihood (REML) implemented in WOMBAT (Meyer 2007). The response variable was the phenotypic scores of each individual in the pedigree on the point estimate of the vector of sexual dimorphism. To test for the presence of additive genetic variation, a likelihood ratio test with one degree of freedom was used to compare the fit of a model that included an additive genetic effect to one that did not.

Cross-sex genetic covariances may not only influence evolutionary trajectories within populations but have the potential to determine how species and sexes diverge from each other over macroevolutionary timescales. We hypothesize that on a macroevolutionary timescale, the most variable sexually dimorphic trait combination may be less constrained by the cross-sex covariances described by **B**, enabling its evolution among species. In contrast, the least variable trait combination may be more constrained by **B**. Here, we focus on the multivariate trait combination that varies the most in sexual dimorphism among 75 species of *Drosophila*, and the multivariate trait combination that varies the least in sexual dimorphism among these same 75 species (Table S2). To determine these multivariate trait combinations, we used a multifactor discriminant approach that we describe in detail in another paper (J. L. Sztepanacz and D. Houle unpubl. data). Briefly, we fit a MANOVA with the 20 wing-shape traits as response variables, and three predictors: a main effect of species, a main effect of sex, and a species*sex interaction. We extracted the sums-of-squares and cross product matrices for the species-by-sex interaction (**H**) and the residual (**E**). The eigenvectors of the matrix $\mathbf{E}^{-1}\mathbf{H}$ describe the multivariate trait combinations that vary in sexual dimorphism among species. The leading eigenvector is the multivariate trait combination that varies the most in sexual dimorphism among species, and the last eigenvector is the trait combination that varies the least.

ESTIMATION OF GENETIC COVARIANCE MATRICES

The genetic variance-covariance matrix of the 20 variable principal component traits was estimated separately for each sex (males: $\mathbf{G}_m$, females: $\mathbf{G}_f$) using REML implemented in WOMBAT. Each trait was multiplied by 1,000 prior to analyses to aid in model convergence. The multivariate linear model was:

$$\mathbf{y} = \mathbf{X}\beta + \mathbf{A}\sigma_A^2 + \mathbf{I}\sigma_E^2, \quad (1)$$

where **y** is the vector of phenotypic observations of all individuals for all traits, **X** is a design matrix relating observations to fixed effects β, **A** is a design matrix relating observations to the additive genetic effects *A*, and **I** is an identity matrix relating observations to the vector of residual effects *E*. The fixed effects were experimental block and trait. Random effects were assumed to be normally distributed and elements of *A* were further assumed to be drawn from $A \sim N(0,\ \mathbf{G} \otimes \mathbf{A})$ where **G** is the additive genetic covariance matrix for the 20 traits and **A** is the numerator relationship matrix. Elements of *E* were assumed to be drawn from $E \sim N(0,\ \mathbf{R} \otimes \mathbf{I})$ where **R** is the residual covariance matrix and **I** is an identity matrix. The dimensionality of each covariance matrix $\mathbf{G}_m$ and $\mathbf{G}_f$ was determined using log-likelihood ratio tests for nested reduced rank models (Hine and Blows 2006), and Akaike's Information Criterion corrected for small sample size (AICc). To formally determine whether $\mathbf{G}_m$ and $\mathbf{G}_f$ differed from each other, we fit the multivariate linear model from Equation (1). However, we fixed the starting values of $\mathbf{G}_m$ at the best estimate of $\mathbf{G}_f$ and maximized the likelihood of the model with respect to these fixed values. A log-likelihood ratio test was used to compare the likelihood of this constrained model with the unconstrained true estimate of $\mathbf{G}_m$. The likelihood ratio test had 210 degrees of freedom, the difference in the number of parameters that were free to vary between models.

Sampling distributions for each covariance component in $\mathbf{G}_m$ and $\mathbf{G}_f$ were obtained using the REML-MVN approach (Meyer and Houle 2013; Houle and Meyer 2015) that samples normal

deviates from the inverse of the Fisher Information matrix. We sampled the elements of the Cholesky factors of the inverse of the Fisher Information matrix (the "L-scale") at the same rank as the best estimate of $\mathbf{G}_m$ or $\mathbf{G}_f$ and used those to construct samples of $\mathbf{G}_m$ or $\mathbf{G}_f$. The sampling distributions of matrices and their functions obtained using this approach are analogous to the posterior distributions obtained from MCMC models and can be interpreted in the same way. Sampling on the L-scale constrains the samples to be positive semi-definite (i.e., variances are bounded by 0) (Houle and Meyer 2015). Therefore, it is not appropriate to compare confidence intervals (CIs) of variances or eigenvalues to 0. Interpreting confidence intervals of variances without reference to an appropriate null distribution can result in erroneous conclusions for the presence of significant variance (Sztepanacz and Blows 2017). However, individual covariances are unbounded, and therefore, the confidence intervals of these parameters can be directly compared to zero. Additionally, the confidence intervals of variances and covariances from $\mathbf{G}_m$ and $\mathbf{G}_f$ can be directly compared to each other.

The same multivariate linear model described in Equation (1) was used to estimate the 40-dimensional genetic covariance matrix $\mathbf{G}_{mf}$, except that each sex-trait combination was treated as a different trait, resulting in 40 traits in the analysis. Because male and female traits are measured on different individuals there is no residual covariance between them, and therefore, elements relating to this part of the matrix were fixed at zero. Consequently, the model estimated 820 parameters for the additive genetic random effect and 420 parameters for the residual. The dimensionality of the 40-trait genetic covariance matrix, $\mathbf{G}_{mf}$ was determined using log-likelihood ratio tests for nested reduced rank models and by AICc values. Sampling distributions for each covariance component in $\mathbf{G}_{mf}$ were obtained by REML-MVN sampling on the L-scale at the same rank as the best estimate of $\mathbf{G}_{mf}$.

CROSS-SEX (CO)VARIANCES

The additive genetic covariance matrix $\mathbf{G}_{mf}$, estimated in the 40-trait analysis, can be viewed as three submatrices: the genetic covariance among traits in males ($\mathbf{G}_m$ submatrix), the genetic covariance among traits in females ($\mathbf{G}_f$ submatrix), and the cross-sex covariances of the traits (**B** submatrix). **B** reflects the degree to which homologous traits in males and females share genetic (co)variance. The diagonal elements of **B** are the between-sex genetic covariance for the same trait. The magnitude of covariance can intuitively be standardized as a correlation. A correlation of zero means that selection on a given trait in one sex should have no impact on that trait in the other sex. A correlation of one means that selection to increase the trait value in one sex will result in a correlated response to increase the trait value in the other. The off-diagonal elements of **B** ($\mathbf{B}_{upper}$ and $\mathbf{B}_{lower}$) are the between-sex covariances for one trait in males and a different trait in females. Their correlations similarly indicate the magnitude of average genetic relationship between the two traits when they are expressed in different sexes. **B** is not necessarily symmetric, so $\mathbf{B}_{upper}$ and $\mathbf{B}_{lower}$ may differ. Asymmetry in **B** can arise due to sex differences in allele frequencies, additive and dominance effects (Fry 2009), or sex-specific gene expression (Allen et al. 2018). To determine whether the correlation between wing-shape traits in males and females resulted in asymmetric patterns of genetic variance between the sexes, we extracted the symmetric and skew-symmetric components of **B** that are uncorrelated with each other using the matrix decomposition:

$$\mathbf{A} = \mathbf{S} + \mathbf{N}, \tag{2}$$

where $\mathbf{S} = 1/2(\mathbf{A} + \mathbf{A}')$ is symmetric and $\mathbf{N} = 1/2(\mathbf{A} - \mathbf{A}')$ is skew symmetric (Gosden and Chenoweth 2014). We then calculated the sums-of-squares of the skew symmetric (**N**) and symmetric (**S**) components, using the percentage of the skew-symmetric sums of squares as the measure of asymmetry, following Gosden and Chenoweth (2014). We applied this decomposition to the point estimate of $\mathbf{G}_{mf}$ and to each of the 1000 RML-MVN samples of $\mathbf{G}_{mf}$, to obtain the 95% confidence intervals.

PARTITIONING $\mathbf{G}_{mf}$ INTO SEXUALLY CONCORDANT AND ANTAGONISTIC GENETIC VARIATION

To quantify the amount of genetic variation that would allow males and females to respond to completely sexually concordant versus completely sexually antagonistic selection, we partitioned our estimate of $\mathbf{G}_{mf}$ into two complementary subspaces: a 20-dimensional subspace with only sexually concordant genetic variation and a 20-dimensional subspace with only sexually antagonistic genetic variation. This partition, thus, characterizes variation allowing a response to selection in exactly the same direction between the sexes and in exactly opposite directions.

Our first step was to construct an arbitrary set of orthonormal vectors ($\mathbf{S}_m$) that spanned the concordant and antagonistic subspaces of $\mathbf{G}_{mf}$. We used the set of 20 eigenvectors $\mathbf{E}_m$ that span the space of a 20-dimensional identity matrix, and divided them by the square root of two, such that S_m (defined below) was orthonormal. We could have equally chosen the set of 20 orthonormal vectors that form the basis for any 20-dimensional matrix and obtained the same result. In the 40 × 40 matrix $\mathbf{S}_\mathrm{m} = \begin{bmatrix} \mathbf{E}_m & \mathbf{E}_m \\ \mathbf{E}_m & -\mathbf{E}_m \end{bmatrix}$, the unit-length vectors in first 20 columns span the space of all concordant genetic variance in $\mathbf{G}_{mf}$, while the unit vectors in columns 21–40 span the space of all antagonistic genetic variance in $\mathbf{G}_{mf}$. We next projected $\mathbf{G}_{mf}$ onto this space

$$\mathbf{G}_{CA} = {\mathbf{S}_m}^T \mathbf{G}_{mf} \mathbf{S}_m, \tag{3}$$

The upper left submatrix of $\mathbf{G}_{CA}$ is a 20-dimensional covariance matrix, $\mathbf{G}_C$, in the concordant subspace while the lower

right submatrix, $\mathbf{G}_A$, is a 20-dimensional covariance matrix in the antagonistic subspace. The trace of $\mathbf{G}_C$ and the trace of $\mathbf{G}_A$ give the total concordant and antagonistic genetic variance in $\mathbf{G}_{mf}$, respectively.

CONSTRAINTS IN THE PREDICTED RESPONSE TO SELECTION DUE TO B

To determine how cross-sex genetic covariances, given by the **B** submatrix of $\mathbf{G}_{mf}$, may constrain the response to selection, we used a modified random skewers approach (Cheverud 1996; Cheverud and Marroig 2007) in conjunction with an extended version of the R metric proposed by Agrawal and Stinchcombe (2009) to determine how much covariances alter the rate of adaptation. This enabled us to identify regions of phenotypic space predicted to have differential responses to selection depending on both the type of selection and covariance the structure of **B**.

The R metric (Agrawal and Stinchcombe 2009) quantifies how much covariances alter the rate of adaptation as the ratio of the predicted response to selection when covariances are included in the breeder's equation versus excluded from the equation. We employed this approach by comparing the predicted response to selection for an estimated $\mathbf{G}_{mf}$ matrix, to one where the entire **B** (**B'**) submatrix of that $\mathbf{G}_{mf}$ is set to 0 (Cox et al. 2017; Holman and Jacomb 2017):

$$R_B = \frac{\beta' \mathbf{G}_{mf} \beta}{\beta' \mathbf{G}_{mf_{(B=0)}} \beta}. \tag{4}$$

We also extended this approach by decomposing **B** into three components that may impact the predicted response to selection differently. In all cases, we changed **B** and **B'** for each of the 1,000 samples of our observed 40-dimensional $\mathbf{G}_{mf}$ matrix. First, we modified **B** so that it was symmetric, replacing the observed **B** with its symmetric component from Equation (2), $\mathbf{G}_{mf_{(B=symmetric)}}$. Second, we removed the remaining symmetric off-diagonal elements of **B** (**B'**) by making them 0, while keeping the diagonal elements at their observed values, $\mathbf{G}_{mf_{(B=diagonal)}}$. This allowed us to test how much of the observed response to selection was facilitated or constrained by cross-sex covariances among different traits. Finally, we set the entire **B** (**B'**) to 0. These modifications of **B** are nested within each other, and therefore, satisfy the following equation:

$$\begin{aligned}\log\left(\frac{\beta' \mathbf{G}_{mf} \beta}{\beta' \mathbf{G}_{mf_{(B=0)}} \beta}\right) &= \log\left(\frac{\beta' \mathbf{G}_{mf} \beta}{\beta' \mathbf{G}_{mf_{(B=symmetric)}} \beta}\right) \\ &+ \log\left(\frac{\beta' \mathbf{G}_{mf_{(B=symmetric)}} \beta}{\beta' \mathbf{G}_{mf_{(B=diagonal)}} \beta}\right) + \log\left(\frac{\beta' \mathbf{G}_{mf_{(B=diagonal)}} \beta}{\beta' \mathbf{G}_{mf_{(B=0)}} \beta}\right).\end{aligned} \tag{5}$$

We calculated each term of Equation (5) to quantify how much each feature of **B** alters the predicted response to selection.

Sometimes our modifications of **B** resulted in the matrices having negative eigenvalues; in these cases, the resulting matrix was bent to the nearest positive definite matrix using the nearPD function (Bates and Maechler 2018) in R (R Core Team 2019). Because the negative eigenvalues were generally of small magnitude the bending did not appear, from visual inspection, to qualitatively change any other aspects of the matrices.

To generate the random skewers, we sampled random 20 element vectors from a multivariate normal distribution $N(0, 1)$. To make a 40-dimensional sexually concordant selection gradient, we stacked a copy of each vector on top of itself. To make a 40-dimensional sexually antagonistic selection gradient, we stacked the opposite of each vector on top of itself. Each vector was scaled to unit length before any subsequent analyses.

We randomly sampled 8,000 selection gradients for each type of selection. Eight thousand was chosen to adequately sample the multivariate space and maintain a reasonable computation time. We projected each selection gradient through each of the 1,000 samples of $\mathbf{G}_{mf}$ and each of the three modified matrices. The genetic variance in the direction of β, which we call the evolvability of β, was determined using the formula

$$\sigma^2_\beta = \beta' \frac{1}{2} \mathbf{G}_{mf} \beta, \tag{6}$$

with the factor of 1/2 to account for the equal autosomal contribution of males and females (Lande 1980). For each selection gradient, we applied Equation (5) to determine the effect of each feature of **B** on the predicted response to selection in that direction.

CONSTRAINTS TO PREDICTED SELECTION RESPONSE IN THE DIRECTION OF SEXUAL DIMORPHISM

To test how **B** would bias the predicted response to selection in the direction of extant sexual dimorphism within *D. melanogaster* and in the genus *Drosophila*, we calculated the predicted response to selection for selection vectors that correspond to these directions for $\mathbf{G}_{mf}$ and for the modified **G**s. The direction of extant sexual dimorphism in *D. melanogaster* is the multivariate trait combination obtained from the linear discriminant function that best separates males and females. We also estimated the directions of greatest and least variation in sexual dimorphism across the *Drosophila* phylogeny (J. L. Sztepanacz and D. Houle unpubl. data). For all three trait combinations, we resampled the data 500 times at the species level and estimated the vectors for each resampled data set, to obtain the sampling error in the estimates. For each estimate of each vector, we created concordant and antagonistic selection vectors as described above. Each vector was then projected through the 1000 samples of our observed and modified **G**s as above. Therefore, the predicted response to selection in each direction incorporates both the sampling error in the estimation

of each selection gradient and the sampling error in the estimate of $\mathbf{G}_{mf}$.

Results

SEXUAL DIMORPHISM

A linear discriminant analysis showed that mean wing shape in *D. melanogaster* was sexually dimorphic. The discriminant function was accurate; crossvalidation correctly predicted sex 95.8% of the time across 1000 unique test data sets that were each comprised of 10% of the total data. The difference in mean wing-shape between males and females was also statistically significant (MANOVA: Pillai's trace = 0.754, $F_{20,\ 17179} = 2643$, $P < 0.0001$), and we found significant additive genetic variation in multivariate sexual dimorphism ($V_{A=}$ 0.363 ± 0.022; $\chi^2 = 2245.914$, $df = 1$, $P < 0.001$) with a heritability of sexual dimorphism of 0.37. To visualize dimorphism in the original traits, we compared the wing-shape defined by the 12 *x*- and *y*-coordinates of the average female wing to the average male wing. The average female wing was contracted in the distal wing tip and expanded in the proximal interior region (Fig. 1). This reflects the fact that the long veins are closer at the tip of the wing and the crossveins are shifted distally in females. The Euclidian distance between males and females in shape space was 15 centroid-size units. This magnitude of shape dimorphism is moderate compared to the range of four to 24 centroid-size units that we have found across 83 species of *Drosophila* (J. L. Sztepanacz and D. Houle unpubl. data). Sexual dimorphism in centroid size, which is a measure of wing-size, was 0.16 when calculated using the sexual dimorphism index $\left(\frac{\text{female size}}{\text{male size}} - 1\right)$. This is comparable to the magnitude of sexual size dimorphism for many traits in many species, as reviewed in Poissant et al (2009).

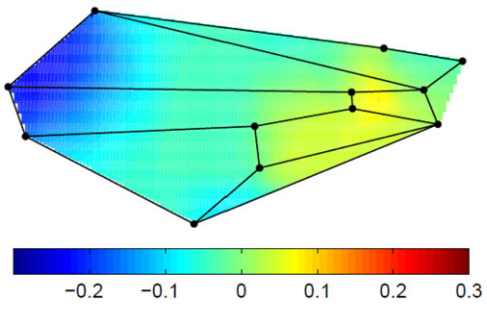

Figure 1. The pattern of relative expansion and contraction in the average wing of females compared to males of *D. melanogaster*. The colors represent the proportional local change in area on the $\log_2$ scale, where the orange value at +0.2 represents an expansion of 15% and the blue value at −0.2 represents a contraction of 15%. Patterns of expansion and contraction are shown in centroid size units for the original *x* and *y* landmark coordinates.

$\mathbf{G}_{mf}$

Male and female **G** matrices were each estimated to have genetic variance in all 20 dimensions of phenotype space, when estimated separately. Fitting 19 variable dimensions significantly reduced the fit of both models: (males $\chi^2 = 6.508$, $df = 1$, $P = 0.01$; females $\chi^2 = 11.85$, $df = 1$, $P < 0.001$). These likelihood ratio results were supported by AICc values that similarly indicated a best fit for 20 dimensions in males (ΔAICc = 2.25) and 20 in females (ΔAICc = 4.92). These results suggest that wing-shape should be able to respond to selection in any direction in both sexes. They are consistent with an analysis of this population that found significant genetic variation in all directions of phenotype space when the male and female data were pooled (Houle and Meyer 2015), and with wing-shape analyses of male *Drosophila serrata* (Sztepanacz and Blows 2015). We compared the fit of the model that estimated $\mathbf{G}_m$ to the fit of a model where the (co)variances of $\mathbf{G}_m$ were constrained to equal the best estimate of $\mathbf{G}_f$, to determine whether $\mathbf{G}_m$ and $\mathbf{G}_f$ differed statistically from each other. The constrained model was a significantly poorer fit than the unconstrained model ($\chi^2 = 334.16$, $df = 210$, $P < 0.001$). Therefore, the orientation of genetic variation that is determined by the (co)variance structure of male and female wing-shape traits differs. However, the total genetic variance did not differ between males and females, nor did the average evolvability, nor the average conditional evolvability (Table 1), suggesting that males and females had equal evolutionary potential overall.

The 40-trait analysis that simultaneously estimated the additive genetic covariance in wing-shape within and between the sexes ($\mathbf{G}_{mf}$) provided a strikingly different picture of genetic variation in wing-shape. Both likelihood ratio tests and AIC values indicated that only 26 of the possible 40 variable dimensions of $\mathbf{G}_{mf}$ had significant additive genetic variance. Reducing dimension from 26 to 25 significantly reduced the fit of the model: ($\chi^2 = 24.95$, $df = 14$, $P = 0.035$; ΔAICc: 0.921). The distribution of genetic variation, given by the eigenvalues of $\mathbf{G}_{mf}$, dropped off after the 20th eigenvalue (Fig. 2), demonstrating that the **B** matrix generates significant genetic constraints. The majority of the genetic variance for the same wing-shape traits in males and females is shared between the sexes, as the genetic correlations between the same wing-shape traits in males and females were approximately 0.9 in all cases (Table 2, Tables S3 and S4).

We partitioned **B** into its upper triangle ($\mathbf{B}_{upper}$) and lower triangle ($\mathbf{B}_{lower}$) components, excluding the diagonal elements, to characterize the asymmetry in **B**. The only difference between $\mathbf{B}_{upper}$ and $\mathbf{B}_{lower}$ is which sex is expressing which trait in the cross-sex covariance estimate. The mean magnitude of covariance did not differ between $\mathbf{B}_{upper}$ and $\mathbf{B}_{lower}$, nor did the average covariance. The point estimates for each covariance component were

Table 1. The total genetic variance in wing shape (V_A) for males and females separately, the average evolvability ($\bar{e}$), and the average conditional evolvability ($\bar{c}$).

	V_A	$\bar{e}$	$\bar{c}$
Male	216.470 (204.930, 228.980)	10.083 (10.246, 11.449)	1.609 (1.501, 1.725)
Female	212.134 (195.937, 216.665)	10.324 (9.979, 10.833)	1.539 (1.428, 1.659)

Confidence intervals (95%) of the estimates are given in parentheses, and were obtained from 1,000 REML-MVN samples of full-rank models sampled on the L-scale.

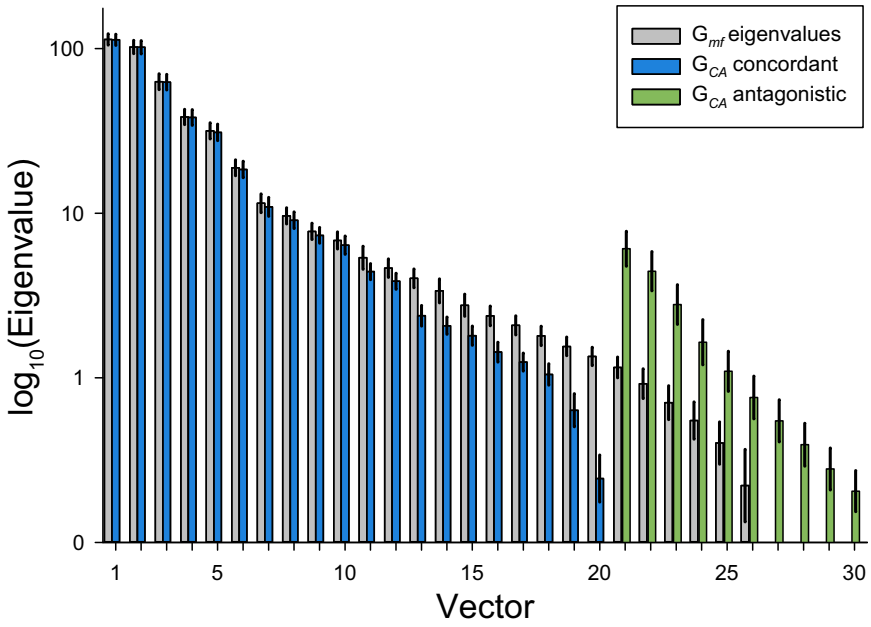

Figure 2. The additive genetic variance in each of the eigenvectors of G_{mf} and the concordant and antagonistic subspaces of G_{CA}. The heights of the bar represents the point estimate of V_A for each eigenvector, and the error bars show the 95% confidence interval of the estimate from REML-MVN sampling on the L-scale of a reduced-rank 26 dimensional model. The first 20 basis vectors of G_{CA} are eigenvectors in the concordant subspace, while the second 20 eigenvectors (only first 10 are shown) are in the antagonistic subspace.

often close to and not significantly different from 0 (Fig. 3). As a result, the sign of the point estimates of $\mathbf{B}_{upper}$ and $\mathbf{B}_{lower}$ were often discordant (91 of 190 had different signs). The proportion of **B** that was skew symmetric was 0.0526 (95% CI: 0.044, 0.113), and was significantly different from zero.

CONCORDANT AND ANTAGONISTIC GENETIC VARIATION IN G_{mf}

We projected $\mathbf{G}_{mf}$ onto concordant and antagonistic subspaces, and just 4.32% (95% CI: 4.31–4.34%) of the total genetic variation lied in the antagonistic subspace. Therefore, the majority of genetic variance in $\mathbf{G}_{mf}$ was sexually concordant, meaning that there is relatively little standing genetic variation that would allow changes in sexual dimorphism. Figure 2 compares the eigenvalues of the 26 eigenvectors of $\mathbf{G}_{mf}$ that have genetic variation with the eigenvalues of concordant ($\mathbf{G}_C$) and antagonistic ($\mathbf{G}_A$) genetic variation. In all cases, the eigenvalues of $\mathbf{G}_{mf}$ were larger than the concordant variance of the same rank. The differences are too small to be apparent for the first few, highly ranked, eigenvectors, but are quite apparent for the low-ranking eigenvectors of $\mathbf{G}_{mf}$. The most variable parts of the antagonistic subspace have more genetic variation than the last 10 dimensions of the concordant subspace. Therefore, the first few eigenvectors of $\mathbf{G}_{mf}$ largely capture concordant variation, and subsequent eigenvectors reflect increasing proportions of antagonistic variation. It is likely that most genetic variants have both concordant and antagonistic effects.

THE EFFECT OF G_{mf} ON EVOLVABILITY

We predicted the response to random direction of selection (e.g., Cheverud and Marroig 2007), and compared the predicted responses based on the full matrix ($\mathbf{G}_{mf}$) to responses predicted by three altered **B** matrices. The three modified matrices (1) replaced **B** with its symmetric component; (2) included only the diagonal of

Table 2. An abbreviated representation of the additive genetic covariance matrix G_{mf} estimated from Equation (1).

	PC1	PC2	PC3	PC4	PC5	...	PC20	PC21	PC22	PC23	PC24	PC25	...	PC40
PC1	**48.430**	*0.093*	*−0.267*	*−0.449*	*−0.234*	...	*0.035*	***0.911***	*0.005*	*−0.283*	*−0.437*	*−0.151*	...	*0.011*
PC2	4.696	**53.087**	*0.092*	*0.088*	*0.039*	...	*0.023*	*0.081*	***0.933***	*0.061*	*0.044*	*0.039*	...	*0.014*
PC3	−10.728	3.869	**33.354**	*−0.030*	*−0.053*	...	0.064	*−0.267*	*0.080*	***0.940***	*−0.038*	*−0.072*	...	*−0.027*
PC4	−14.337	2.940	−0.789	**21.063**	*0.027*	...	*0.012*	*−0.366*	*0.099*	*0.010*	***0.907***	*−0.043*	...	*−0.037*
PC5	−7.007	1.229	−1.310	0.524	**18.473**	...	*−0.005*	*−0.191*	*0.083*	*−0.019*	*0.029*	***0.934***	...	*0.040*
...	|	|	|	|	|	...	|	|	|	|	|	|	...	|
PC20	0.106	0.072	0.159	0.024	−0.010	...	**0.187**	*0.023*	*0.052*	*0.103*	*0.127*	*0.032*	...	***0.858***
PC21	**39.981**	3.725	−9.736	−10.585	−5.167	...	0.023	**39.809**	*0.008*	*0.016*	*0.038*	*0.063*	...	*0.858*
PC22	0.277	**49.663**	3.369	3.330	2.607	...	0.052	−0.424	**53.419**	*−0.009*	*−0.356*	*−0.371*	...	*0.036*
PC23	−12.261	2.760	**33.791**	0.291	−0.501	...	0.103	−13.964	4.738	**38.739**	*0.104*	*0.110*	...	*−0.039*
PC24	−14.240	1.491	−1.037	**19.516**	0.587	...	0.127	−10.973	3.757	−0.590	**21.960**	*−0.020*	...	*−0.061*
PC25	−4.431	1.194	−1.755	−0.827	**16.892**	...	0.032	−3.430	2.228	−0.733	−2.329	**17.689**	...	*0.015*
...	|	|	|	|	|	...	|	|	|	|	|	|	...	|
PC40	0.038	0.049	−0.074	−0.081	0.082	...	**0.175**	0.109	−0.136	−0.179	0.034	0.085	...	**0.224**

PC1 to PC20 are the 20 male wing-shape traits and PC21 to PC40 are the 20 female wing-shape traits. The top left and bottom right quadrants represent the symmetric G_m and G_f portions of G_{mf}, respectively, with covariances given in the lower triangle of the submatrices and correlations given in italics in the upper triangle. Genetic variances are shown on the diagonal in bold. The bottom left quadrant represents the asymmetric cross-sex (co)variances (B), with sex-specific variance on the diagonal (in bold) and covariances on the off-diagonal. The top right quadrant expresses the transpose of B as correlations. See Table S3 for the full 40 × 40 G_{mf} matrix, and Table S4 for a 48 × 48 G_{mf} matrix where the principal component traits have been backtransformed to their original *x*-*y* shape coordinates.

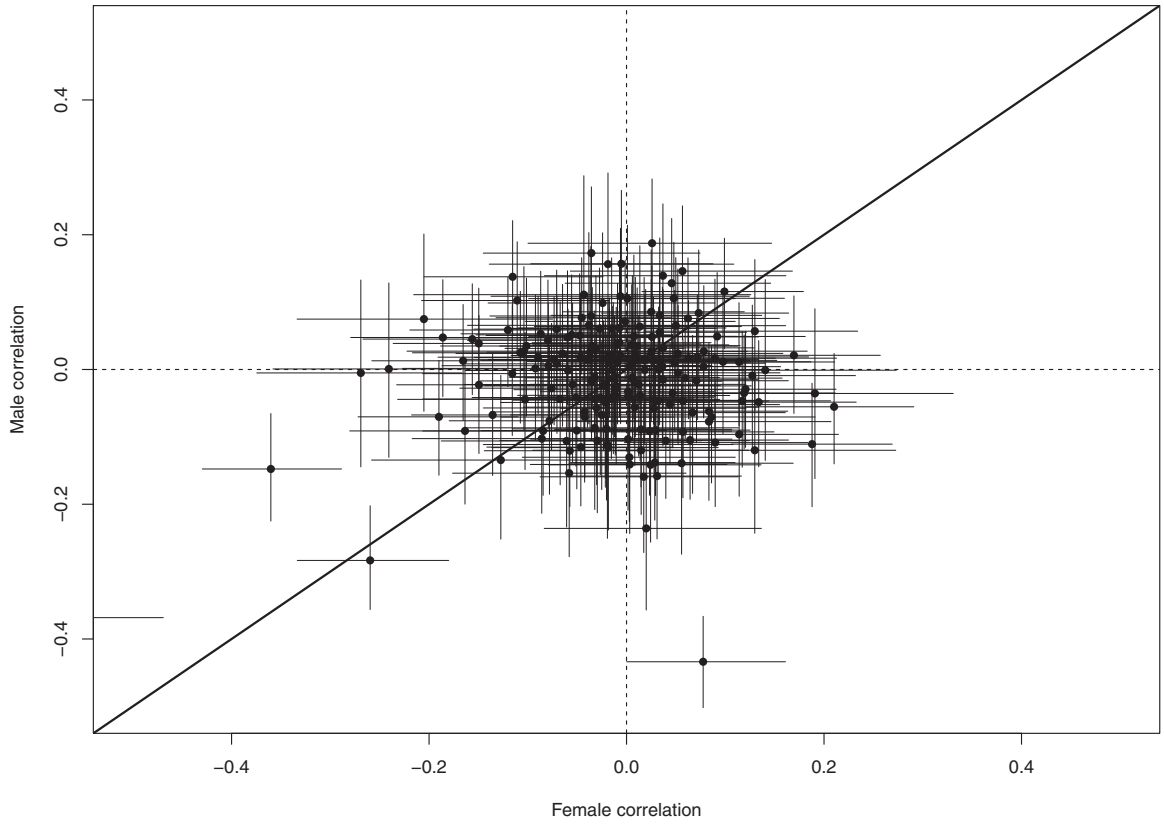

Figure 3. The individual cross-sex correlations of B_{lower} versus B_{upper} for the 20 principal component wing-shape traits. Correlations that fall on the 1:1 line are symmetric, whereas those that do not are asymmetric cross-sex cross trait correlations. Points in the top right and bottom left quadrants are correlations that are asymmetric in magnitude but not sign, whereas those in the bottom right and top left quadrants are asymmetric in both sign and magnitude. Each point represents the point estimate of the correlation with bars that represent the 95% confidence intervals from 1000 REML-MVN samples on the L-scale of a reduced-rank 26-dimensional model of G_{mf}.

B; and (3) set **B** to 0. Results are shown in Table 3. When selection was antagonistic, **B** decreased the predicted response to selection by over 91% compared to a matrix where **B** was set to 0 so that males and female traits could evolve completely independently. Asymmetry in the covariances of $\mathbf{B}_{upper}$ and $\mathbf{B}_{lower}$ had little effect on the predicted response, accounting for less than 1% of the total constraint imposed by **B**. Symmetric cross-sex crosstrait covariances reduced the response by 27.5%. Cross-sex covariances for the same trait, quantified using a diagonal **B**, accounted for an additional 72% of the total reduction. To test whether the direction of the predicted responses in the two sexes was equal, we calculated the angle between the sex-specific part of the predicted response vector and the sex-specific part of the selection gradient. This takes into account how the sex-specific covariances given by $\mathbf{G}_m$ or $\mathbf{G}_f$ and **B**, together, bias the predicted response to selection. The response was biased by a similar average magnitude in females and males. However, there was notably more variation in the orientation of predicted response vectors in females than in males (Fig. 4A).

The effect of **B** on the predicted response to random directions of selection was markedly different when selection was concordant. **B** facilitated the response to selection by two times, when compared to $\mathbf{B} = 0$, where males and females could evolve independently. The facilitated response was driven entirely by the diagonal elements of **B**. Neither cross-sex cross trait covariances, nor asymmetry in these covariances had any effect on the predicted response to selection (Table 3). For every random selection gradient that we studied, the summed effects of $\mathbf{G}_m$ ($\mathbf{G}_f$) and **B** oriented the predicted response vector away from the selection gradient more in males than in females (Fig. 4B). This reduced the total amount by which **B** could increase the response to selection at the population level.

We also quantified the effect of **B** on the predicted response to selection for three particular multivariate trait combinations that may be subject to selection: (1) the direction of sexual dimorphism in *D. melanogaster* and the direction of (2) greatest variation in sexual dimorphism across the *Drosophila* phylogeny. We contrasted these with (3) the predicted response in the direction

Table 3. The components of **B** that bias the predicted response to constructed vectors of antagonistic and concordant selection, from Equation (5).

Constructed selection vector		$\log(B/B_0)$	Prop. asymmetry	Prop. cross-sex cross trait covariances	Prop. cross-sex covariances
Antagonistic	Random skewers	−1.077 (−1.368, −0.821)	0.00893 (0.00065,0.034)	0.275 (−0.193, 0.604)	0.716 (0.387,1.186)
	D. melanogaster dimorphism	−0.982 (−1.138, −0.830)	0.0149 (0.0031,0.036)	−0.016 (−0.274, 0.194)	1.00 (0.787,1.262)
	Maximum among species variation in dimorphism	−1.081 (−1.138, −0.830)	0.016 (0.002,0.045)	0.010 (−0.356, 0.372)	0.974 (0.604, 1.345)
	Minimum among species variation in dimorphism	−1.021 (−1.138, −0.830)	0.043 (0.0067, 0.107)	0.412 (0.044 ,0.635)	0.545 (0.312,0.921)
Concordant	Random skewers	0.281 (0.267, 0.291)	0.000 (−0.002, 0.000)	−0.019 (−0.377, 0.000)	1.019 (0.802, 1.378)
	D. melanogaster dimorphism	0.278 (0.268, 0.285)	−0.001 (−0.003, 0.000)	−1.192 (−1.135, −1.052)	2.193 (2.053, 2.356)
	Maximum among species variation in dimorphism	0.282 (0.271, 0.291)	0.000 (−0.002, 0.000)	−0.470 (−0.72, −0.100)	1.470 (1.100, 1.721)
	Minimum among species variation in dimorphism	0.279 (0.261, 0.290)	−0.006 (−0.027, 0.000)	0.011 (−0.206, 0.183)	0.996 (0.823, 1.213)

$\text{Log}_{10}(B/B_{=0})$ is the total amount that **B** constrains/facilitates the response. Negative values indicate that **B** constrains the response and positive values indicate that **B** facilitates the response. The proportions are directly comparable to each other and sum to one. Prop. Asymmetry is the proportion of $\text{Log}_{10}(B/B_{=0})$ that is accounted for by asymmetry in **B**, Prop. Cross-sex cross-trait covariances is the proportion accounted for my symmetric off-diagonal elements of **B**, and Prop. Cross-sex covariances is the proportion accounted for by the diagonal elements of **B**. Proportions of different sign than $\text{Log}_{10}(B/B_{=0})$ indicate that that component of **B** has the opposite effect than the total effect of **B**. Values in parentheses denote 95% confidence intervals of each estimate.

of the least variation in sexual dimorphism across the *Drosophila* phylogeny. These three vectors were not highly correlated with each other (Table 4). The response to antagonistic selection was constrained in all three trait combinations by a factor of about 12, similar to the average constraint observed over random directions of selection. The diagonal of **B** accounted for almost all of the constraint in *D. melanogaster* sexual dimorphism and the direction of maximum variation in sexual dimorphism across the *Drosophila* phylogeny (Table 3). The diagonal and symmetric off-diagonal of **B** contributed equally to the constraint that we observed in the direction of minimum variation among species in sexual dimorphism (Table 3). **B** facilitated the total response of each of the three trait combinations by a factor of about 2 when selection was sexually concordant (Table 3). For two trait combinations, one part of **B** facilitated the response and another part of **B** constrained the response. The diagonal of **B** facilitated the response in *D. melanogaster* sexual dimorphism by 200%, and in the direction of maximum variation in sexual dimorphism across the phylogeny by 150%. The symmetric off-diagonal of **B** had the opposite effect, constraining the response by 120% and 50% in each respective trait combination. The diagonal of **B** was the only component to affect the response to selection in the direction of minimum variation in sexual dimorphism among species.

Discussion

Genetic covariances among traits have an important role in biasing both the direction and magnitude of response to selection. Cross-sex genetic covariances are of particular interest, because they determine whether and to what extent sexual dimorphism can evolve when the optimal trait values of males and females differ. Although there are many estimates of intersexual genetic correlations for single traits (Poissant et al. 2009), multivariate estimates of cross-sex covariances are less common (Wyman et al. 2013). Here we demonstrate, for multivariate wing-shape phenotypes of *D. melanogaster,* that cross-sex genetic covariances characterized by the **B** matrix significantly bias the predicted responses to multivariate selection. We show that cross-sex covariances reduce the predicted response to divergent selection (1) in random directions, (2) in the direction of extant sexual dimorphism in *D. melanogaster,* and (3) in directions of most and least variation in sexual dimorphism over macroevolutionary timescales. We also found that **B** can increase the response to sexually concordant selection, but in a complex way that is determined by the interaction of different parts of **B**. The diagonal elements of **B** increased the predicted response, while the off-diagonal elements of **B** simultaneously reduced it, but to a lesser extent. Furthermore, the summed effects of diagonal and off-diagonal elements biased the predicted response to selection differently in males and females, and in such a way that suggests males may

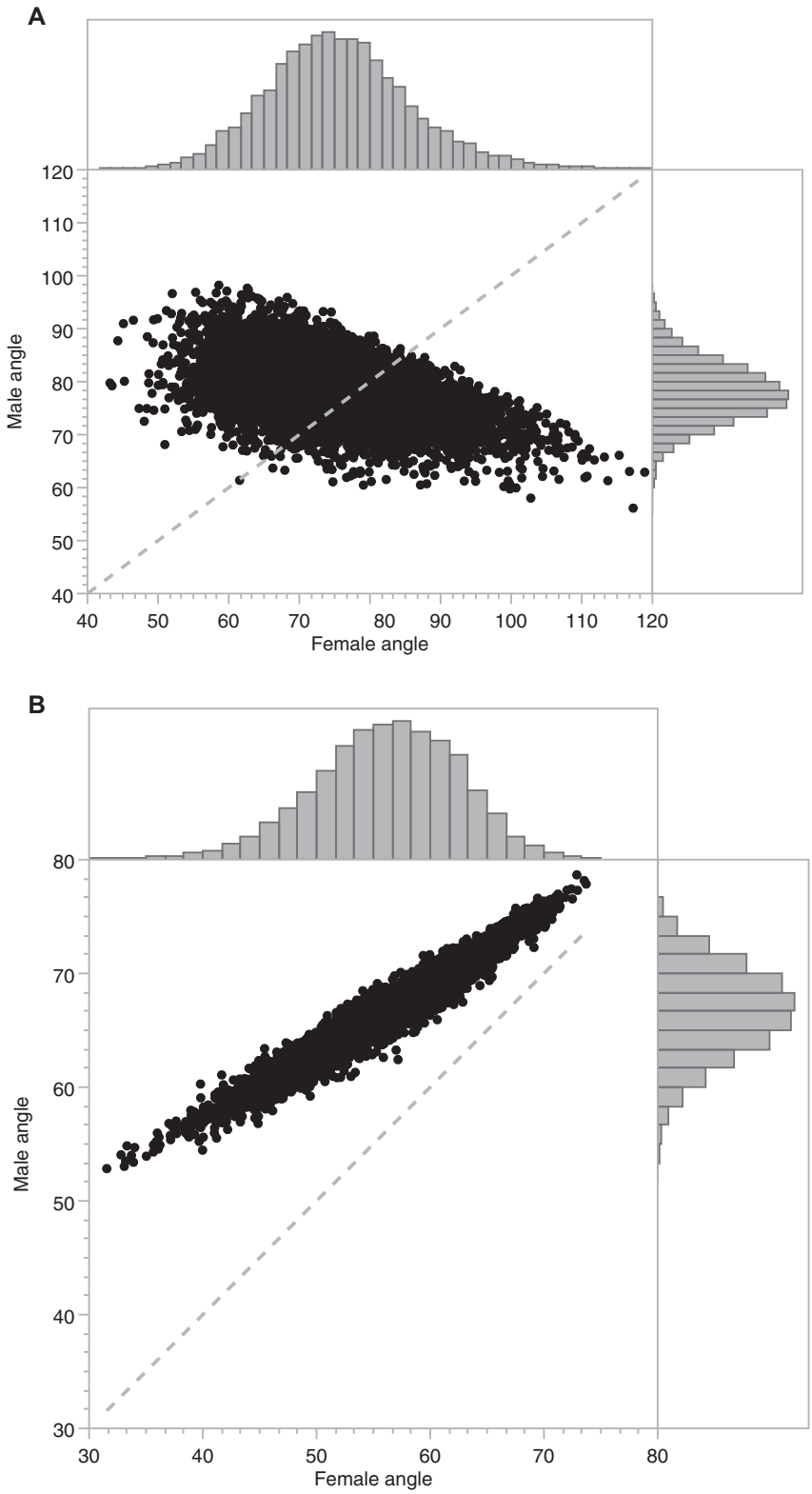

Figure 4. **(A) The angles (in degrees) between the sex-specific predicted response to antagonistic selection and the sex-specific selection gradient. There are 8,000 data points, one for each random skewer. The dashed line shows a 1:1 relationship between males and females. Histograms denote the variance in angles for each sex, note the larger variance in female angle compared to male angle. (B) The angles (in degrees) between the sex-specific predicted response to concordant selection and the sex-specific selection gradient. There are 8,000 data points, one for each random skewer. The dashed line shows a 1:1 relationship between males and females. Note that for every selection gradient, the response is biased away from the selection gradient more in males than in females.**

Table 4. Vector correlations between the directions of *D. melanogaster* sexual dimorphism, maximum, and minimum, variation in sexual dimorphism among 75 *Drosophila* species.

Trait Vectors	Sexual dimorphism	Maximum variation among species	Minimum variation among species
SD	0.0055	0.11	0.27
Sexual dimorphism	*1.000*	*−0.112*	*−0.249*
Maximum variation among species		*1.000*	*−0.077*
Minimum variation among species			*1.000*

SD indicates the standard deviation of the angles between the point estimate of each vector and the 500 bootstrapped samples of each vector. The vectors were scaled to unit length and are presented in Table S2.

experience stronger evolutionary constraints than females. Our results suggest that when both sexes are considered in evolutionary predictions, *Drosophila* wings may not be evolvable in all directions of phenotype space, in contrast with the results from single-sex analyses. Cross-sex covariances may, therefore, provide one explanation for the remarkable stability of wing-shape phenotypes observed across macroevolutionary timescales.

The response to sexually divergent selection may be strongly constrained by cross-sex correlations. Therefore, many studies to examine a role of single ($\boldsymbol{r}_{mf}$) or multivariate (**B**) cross-sex correlations in biasing responses to selection, have focused on qualitatively dimorphic traits that are known to have a role in sexual selection. How selection acts on wing-shape in *Drosophila* is generally unknown; however, there is some evidence that male wings of *D. melanogaster* are subject to sexual selection to increase their length. For example, males collected from the field that were engaged in mating had longer wings than those that were not (Taylor and Kekic 1988), and artificial selection to increase wing length conferred a mating advantage to males, after controlling for correlated differences in body size (Menezes et al. 2013). Consistent with these studies, we found *D. melanogaster* wing-shape to be significantly sexually dimorphic with the size-adjusted distal portion of the wing tip longer in males than females (Fig. 1). We cannot definitively say whether the magnitude of sexual dimorphism in wing-shape that we observed was biologically meaningful; however, it was in the middle of sexual dimorphism magnitudes observed for 83 species of *Drosophila* (J. L. Sztepanacz and D. Houle unpubl. data).

The cross-sex genetic correlations for single wing-shape traits in males and females ($\boldsymbol{r}_{mf}$) were all positive and of a large magnitude, reflecting the shared genetic and developmental (Matamoro-Vidal et al. 2018) basis of wings in males and females, and consistent with the low qualitative dimorphism in wings. Previous studies have established that higher cross-sex correlations tend to be associated with lower dimorphism, and that most estimates of $\boldsymbol{r}_{mf}$ are large and positive (Poissant et al. 2009). In particular, morphological traits tend to have higher cross-sex correlations and lower dimorphism than fitness components. Our estimates for wing-shape phenotypes are consistent with these observations and with a largely shared genetic architecture of wing-shape between males and females. Sex-specific selection is also predicted to generate dimorphism in the additive genetic variance and covariance structure of sexually dimorphic traits. Wyman and Rowe (2014) found a weak ($\rho = 0.19$) positive relationship between dimorphism in additive genetic variances and dimorphism in trait means in a review of 252 estimates from 75 species. This relationship was based on single-trait estimates only. Punzalan and Rowe (2015) compared the multivariate phenotypic covariance structure of three traits among seven congeneric insect species. They found that sexual dimorphism in trait means positively covaried with dimorphism in the major axis of phenotypic covariance, providing further support for a relationship between sexual dimorphism in trait means and dimorphism in genetic variance. Consistent with the relatively low level of sexual dimorphism that we observed in wing-shape, we did not find any significant difference in additive genetic variance between the sexes for any individual wing-shape traits (Table 2, Table S3).

Our results also showed that $\mathbf{G}_m$ and $\mathbf{G}_f$ each had genetic variation in all directions of phenotype space. Full-rank **G** matrices are not typical of multivariate studies (Walsh and Blows 2009) but have been observed for *Drosophila* wing-shape in studies that have particularly large sample sizes (Mezey and Houle 2005; Houle and Meyer 2015; Sztepanacz and Blows 2015). Comparisons of $\mathbf{G}_m$ and $\mathbf{G}_f$ in other species suggest that the amount of genetic variation is often sexually dimorphic, but that the orientation of genetic variation is similar between the sexes (Ashman 2003; Arnold et al. 2008; Barker et al. 2010; Campbell et al. 2011; Wyman et al. 2013). These results may be explained, in part, by a lack of power to detect subtle differences in orientation. Our study has a particularly large sample size of over 17,000 individuals, that allowed us to estimate **G** with high precision. We found that the total genetic variance did not differ between males and females, nor did the average evolvability nor the average conditional evolvability for wing-shape (Table 1). But there was sexual dimorphism in the orientation of genetic variation.

The covariance structure of $\mathbf{G}_m$ and $\mathbf{G}_f$ differed significantly from each other, despite the qualitative similarity between them. This could be a consequence of sex-specific differences in selection, sex differences in mutational (co)variance, or some combination of the two.

The distribution of genetic variation in $\mathbf{G}_{mf}$ that includes cross-sex covariances (**B**) contrasted with what we observed in $\mathbf{G}_m$ and $\mathbf{G}_f$. Only two-thirds of the multivariate trait combinations of $\mathbf{G}_{mf}$ had detectable genetic variation, whereas $\mathbf{G}_m$ and $\mathbf{G}_f$ had genetic variation spanning the entire phenotypic space. Therefore, the region of dimorphic phenotype space seems to be relatively inaccessible to selection. Some of the pattern may also be due to subtle differences in the covariance structure of $\mathbf{G}_m$ and $\mathbf{G}_f$. The effect of **B** in biasing the response to selection was qualitatively predictable: **B** constrained the response to sexually antagonistic selection, and **B** facilitated the response to sexually concordant selection. In *D. serrata,* including the **B** matrix in the predicted response to sexual selection on cuticular hydrocarbon pheromones constrained the predicted response to divergent selection (Gosden et al. 2012; Gosden and Chenoweth 2014), and similar results have been observed in meal moths (Lewis et al. 2011), and for the least sexually dimorphic cuticular hydrocarbons of *D. melanogaster* (Ingleby et al. 2014). In contrast **B** facilitated (Holman and Jacomb 2017) or had limited effect (Walling et al. 2014; Cox et al. 2017) on the predicted response to concordant selection in life-history traits of *Tribolium castaneum,* in multivariate Anole dewlap traits, and in Red Deer, respectively.

The magnitude of bias that we observed was more surprising. The response to antagonistic selection was constrained by 90% on average as a result of the diagonal elements of **B.** The diagonals of **B** had the same effect in limiting divergence in the direction of extant sexual dimorphism in *D. melanogaster,* and in limiting further divergence in sexual dimorphism among species, whereas the symmetric off-diagonal elements of **B** had almost no effect in these directions. This an interesting contrast with the direction of least divergence in sexual dimorphism, where both the diagonal of **B** and the off-diagonal of **B** constrained the response to selection. Selection is predicted to orient the covariance structure of multivariate trait combinations to match the fitness surface (Arnold et al. 2001). Correlational selection has been shown to orient bivariate correlations (Brodie 1992), and Brooks et al (2005) showed that the covariance structure of **G** aligns with the fitness surface for multivariate cricket song. We do not know the form of selection on wing-shape, but the contrasting pattern of constraint that we observed for the most dimorphic compared to the least dimorphic trait combinations could point to a history of divergent selection on the most dimorphic traits that has oriented the off-diagonals of **B** to allow each sex to approach their optimal trait values. The least dimorphic traits may have not been subject to the same divergent selection, which is why we observe that both the diagonal and off-diagonal of **B** constrains their response. For the most dimorphic traits, because all correlational constraints have been resolved, the evolution of further dimorphism would then require a reduction in the diagonal of **B**. This could be achieved through mechanisms such as sex-biased mutational variation (Sharp and Agrawal 2012), sex-specific dominance effects (Fry 2009), genomic imprinting (Day 2004), or sex specific gene expression (Ingleby et al. 2015; Wright et al. 2018). An alternative hypothesis is that the evolution of dimorphism has proceeded in the observed direction because it is the direction least constrained by **B**. Studies that incorporate estimates of selection on wing-shape with **B** will be required to distinguish between these two hypotheses.

We found that **B** facilitated the response to concordant selection overall, but the effect of **B** was complex. The diagonal of **B** facilitated the response, because all values of $\boldsymbol{r}_{\mathrm{mf}}$ approached one, the maximum possible value. The off-diagonal elements of **B** had the opposite effect. The summed effects of $\mathbf{G}_m$ ($\mathbf{G}_f$) and **B** reduced the magnitude of response in a way that prevented males from becoming too female-like, generating a larger angle of deflection between the response vector and selection gradient in males than in females (Fig. 4B). We also saw a difference in sex-specific deflection vectors under concordant selection. The mean magnitude of deflection was similar between the sexes, but there was much more variation in females (Fig. 4A). Together, these results suggest that evolutionary constraints are stronger for males than for females. Studies in other *Drosophila* species have demonstrated that wing-shape in males experiences stabilizing selection through pleiotropic fitness costs of unknown but correlated traits (McGuigan et al. 2011; Sztepanacz et al. 2017). One study has also demonstrated a higher rate of mutational variance in male wings than female wings (Carreira et al. 2011), although another study found no difference (Houle and Fierst 2013). We observed similar levels of standing genetic variance in males and females. One explanation of these results could be that the unknown correlated traits resulting in apparent stabilizing selection on male wings are wing traits in females. Whether selection for dimorphism determines the genetic (co)variation captured in **B**, or whether **B** dictates the patterns of dimorphism that we observe within and across species is the key question that must be answered to understand whether cross-sex covariances generate long-term evolutionary constraints. To begin to answer this question we need to understand, in a sex-specific way, how mutational variation is translated into standing genetic variation, and how selection acts on this variation.

Previous analyses of these data that pooled the two sexes suggested that evolution was possible in any direction in phenotype space (Houle and Meyer 2015). In this analysis, where we explicitly consider the genetic variation within and between the sexes, the picture is quite different. We have shown that

cross-sex genetic covariances can considerably limit the evolution of male and female phenotypes in response to antagonistic selection, thereby, limiting evolutionary divergence in the direction of extant sexual dimorphism in *D. melanogaster* and across the phylogeny of *Drosophila*. We have also shown that cross-sex covariances can facilitate the response to concordant selection, but in a complex way that moderates divergence between the sexes. Our decomposition of the total effect of **B** into that determined by $\boldsymbol{r}_{mf}$, by cross-sex cross trait covariances, and by asymmetry in genetic variance between the sexes, has shown that the pleiotropic effects of alleles on the same trait in males and females determine the majority of evolutionary constraint. This may not be surprising, considering the relatively low sexual dimorphism in wing-shape when compared to many other traits. Whether our results are unique to our system, or whether they exemplify a more general consequence of males and females inheriting the same alleles from their parents, will only be determined by future studies that partition the effects of **B** into its three components.

AUTHOR CONTRIBUTIONS

J.L.S. and D.H. conceived the project. J.L.S performed the analyses. J.L.S. and D.H. wrote the paper.

ACKNOWLEDGMENTS

We would like to thank Steve Chenoweth and Thomas F. Hansen for helpful comments and suggestions regarding the analyses. We would also like to thank Joel McGlothlin, Dave Punzalan, and one anonymous reviewer for their helpful comments on the manuscript. This research was supported by National Science Foundation grants DEB-0129219 and DEB-1556774.

DATA ARCHIVING

Data is archived in Dryad: https://doi.org/10.5061/dryad.pr996gj.

LITERATURE CITED

Abbott, J. K., S. Bedhomme, and A. K. Chippindale. 2010. Sexual conflict in wing size and shape in *Drosophila melanogaster*. J. Evol. Biol. 23:1989–1997.

Agrawal, A. F., and J. R. Stinchcombe. 2009. How much do genetic covariances alter the rate of adaptation? Proc. Biol. Sci. 276:1183–1191.

Allen, S. L., R. Bonduriansky, and S. F. Chenoweth. 2018. Genetic constraints on microevolutionary divergence of sex-biased gene expression. Philos. Trans. R Soc. B: Biol. Sci. 373:20170427.

Arnold, S. J., M. E. Pfrender, and A. G. Jones. 2001. The adaptive landscape as a conceptual bridge between micro- and macroevolution. Genetica 112:9–32.

Arnold, S. J., R. Bürger, P. A. Hohenlohe, B. C. Ajie, and A. G. Jones. 2008. Understanding the evolution and stability of the G-matrix. Evolution 62:2451–2461.

Ashman, T. L. 2003. Constraints on the evolution of males and sexual dimorphism: field estimates of genetic architecture of reproductive traits in three populations of gynodioecious *Fragaria virginiana*. Evolution 57:2012–2025.

Barker, B. S., P. C. Phillips, and S. J. Arnold. 2010. A test of the conjecture that G-matrices are more stable than B-matrices. Evolution 64:2601–2613.

Barton, N., and L. Partridge. 2000. Limits to natural selection. Bioessays 22:1075–1084.

Bates D. and M. Maechler. 2018. Matrix: Sparse and Dense Matrix Classes and Methods. R package version 1.2-15. https://CRAN.R-project.org/package=Matrix

Blows, M. W., and A. A. Hoffmann. 2005. A reassessment of genetic limits to evolutionary change. Ecology 86:1371–1384.

Bolstad, G. H., J. A. Cassara, E. Márquez, T. F. Hansen, K. van der Linde, D. Houle, and C. Pélabon. 2015. Complex constraints on allometry revealed by artificial selection on the wing of *Drosophila melanogaster*. Proc. Natl. Acad. Sci. 112:13284–13289.

Bonduriansky, R., and S. F. Chenoweth. 2009. Intralocus sexual conflict. Trends Ecol. Evol. 24:280–288.

Brodie, E. D. 1992. Correlational selection for color pattern and antipredator behavior in the garter snake *Thamnophis ordinoides*. Evolution 46:1284–1298.

Brooks, R. R., J. J. Hunt, M. W. M. Blows, M. J. M. Smith, L. F. L. Bussière, and M. D. M. Jennions. 2005. Experimental evidence for multivariate stabilizing sexual selection. Evolution 59:871–880.

Campbell, D. R., S. G. Weller, A. K. Sakai, T. M. Culley, P. N. Dang, and A. K. Dunbar Wallis. 2011. Genetic variation and covariation in floral allocation of two species of *Schiedea* with contrasting levels of sexual dimorphism. Evolution 65:757–770.

Carreira, V. P., I. M. Soto, J. Mensch, and J. J. Fanara. 2011. Genetic basis of wing morphogenesis in *Drosophila*: sexual dimorphism and non-allometric effects of shape variation. BMC Dev. Biol. 11: 32.

Chenoweth, S. F., H. D. Rundle, and M. W. Blows. 2010. The contribution of selection and genetic constraints to phenotypic divergence. Am. Nat. 175:186–196.

Cheverud, J. M. 1996. Quantitative genetic analysis of cranial morphology in the cotton-top (*Saguinus oedipus*) and saddle-back (*S. fuscicollis*) tamarins. J. Evol. Biol. 9:5–42.

Cheverud, J. M., and G. Marroig. 2007. Research article comparing covariance matrices: random skewers method compared to the common principal components model. Genet. Mol. Biol. 30:461–469.

Collet, J. M., S. Fuentes, J. Hesketh, M. S. Hill, P. Innocenti, E. H. Morrow, K. Fowler, and M. Reuter. 2016. Rapid evolution of the intersexual genetic correlation for fitness in *Drosophila melanogaster*. Evolution 70:781–795.

Connallon, T., and A. G. Clark. 2013. Evolutionary inevitability of sexual antagonism. Proc. Biol. Sci. 281:20132123.

Conner, J., and S. Via. 1993. Patterns of phenotypic and genetic correlations among morphological and life-history traits in wild radish, Raphanus *raphanistrum*. Evolution 47:704–711.

Cox, R. M., and R. Calsbeek. 2009. Sexually antagonistic selection, sexual dimorphism, and the resolution of intralocus sexual conflict. American Nat. 173:176–187.

Cox, R. M., R. A. Costello, B. E. Camber, and J. W. McGlothlin. 2017. Multivariate genetic architecture of the *Anolisdewlap* reveals both shared and sex-specific features of a sexually dimorphic ornament. J. Evol. Biol. 30:1262–1275.

Day, T. 2004. Intralocus sexual conflict can drive the evolution of genomic imprinting. Genetics 167:1537–1546.

Delph, L. F., J. C. Steven, I. A. Anderson, C. R. Herlihy, and E. D. Brodie III. 2011. Elimination of a genetic correlation between the sexes via artificial correlational selection. Evolution 65:2872–2880.

Foerster, K., T. Coulson, B. C. Sheldon, J. M. Pemberton, T. H. Clutton-Brock, and L. E. B. Kruuk. 2007. Sexually antagonistic genetic variation for fitness in red deer. Nature 447:1107–1111.

Fry, J. D. 2009. The genomic location of sexually antagonistic variation: some cautionary comments. Evolution 310:119–112.

Gidaszewski, N. A., M. Baylac, and C. Klingenberg. 2009. Evolution of sexual dimorphism of wing shape in the *Drosophila melanogaster* subgroup. BMC Evol. Biol. 9:110.

Gomulkiewicz, R., and D. Houle. 2009. Demographic and genetic constraints on evolution. Am. Nat. 174:E218–E229.

Gosden, T. P., and S. F. Chenoweth. 2014. The evolutionary stability of cross-sex, cross-trait genetic covariances. Evolution 68:1687–1697.

Gosden, T. P., K.-L. Shastri, P. Innocenti, and S. F. Chenoweth. 2012. The B-matrix harbors significant and sex-specific constraints on the evolution of multicharacter sexual dimorphism. Evolution 66:2106–2116.

Hansen, T. F., and D. Houle. 2008. Measuring and comparing evolvability and constraint in multivariate characters. J. Evol. Biol. 21:1201–1219.

Hine, E., and M. W. Blows. 2006. Determining the effective dimensionality of the genetic variance–covariance matrix. Genetics 173:1135–1144.

Hine, E., K. McGuigan, and M. W. Blows. 2014. Evolutionary constraints in high-dimensional trait sets. Am. Nat. 184:119–131.

Hine, E., D. E. Runcie, K. McGuigan, and M. W. Blows. 2018. Uneven distribution of mutational variance across the transcriptome of *Drosophila serrata* revealed by high-dimensional analysis of gene expression. Genetics 209:1319–1328.

Holman, L., and F. Jacomb. 2017. The effects of stress and sex on selection, genetic covariance, and the evolutionary response. J. Evol. Biol. 30:1898–1909.

Houle, D., and J. Fierst. 2013. Properties of spontaneous mutational variance and covariance for wing size and shape in *Drosophila melanogaster*. Evolution 67:1116–1130.

Houle, D., and K. Meyer. 2015. Estimating sampling error of evolutionary statistics based on genetic covariance matrices using maximum likelihood. J. Evol. Biol. 28:1542–1549.

Houle, D., D. R. Govindaraju, and S. Omholt. 2010. Phenomics: the next challenge. Nat. Rev. Genet. 11:855–866.

Houle, D., G. H. Bolstad, K. van der Linde, and T. F. Hansen. 2017. Mutation predicts 40 million years of fly wing evolution. Nature 548:447–450

Houle, D., J. Mezey, P. Galpern, and A. Carter. 2003. Automated measurement of *Drosophila* wings. BMC Evol. Biol. 3:25.

Ingleby, F. C., I. Flis, and E. H. Morrow. 2015. Sex-biased gene expression and sexual conflict throughout development. Cold Spring Harb. Perspect. Biol. 7:a017632

Ingleby, F. C., P. Innocenti, H. D. Rundle, and E. H. Morrow. 2014. Between-sex genetic covariance constrains the evolution of sexual dimorphism in *Drosophila melanogaster*. J. Evol. Biol. 27:1721–1732.

Kirkpatrick, M. 2008. Patterns of quantitative genetic variation in multiple dimensions. Genetica 136:271–284.

Lande, R. 1979. Quantitative genetic analysis of multivariate evolution, applied to brain:body size allometry. Evolution 33:402–416.

———. 1980. Sexual dimorphism, sexual selection, and adaptation in polygenic characters. Evolution 34:292–305.

Lewis, Z., N. Wedell, and J. Hunt. 2011. Evidence for strong intralocus sexual conflict in the Indian meal moth, *Plodia interpunctella*. Evolution 65:2085–2097.

Long, T. A. F., and W. R. Rice. 2007. Adult locomotory activity mediates intralocus sexual conflict in a laboratory-adapted population of *Drosophila melanogaster*. Proc. Soc. Biol. Sci. 274:3105–3112.

Lynch, M., & Walsh, B. 1998. Genetics and analysis of quantitative traits. Sunderland, MA, Sinauer.

Maklakov, A. A., S. J. Simpson, F. Zajitschek, M. D. Hall, J. Dessmann, F. Clissold, D. Raubenheimer, R. Bonduriansky, and R. C. Brooks. 2008. Sex-specific fitness effects of nutrient intake on reproduction and lifespan. Curr. Biol. 18:1062–1066.

Marquez, E. J., R. Cabeen, R. P. Woods, and D. Houle. 2012. The measurement of local variation in shape. Evol. Biol. 39:419–439.

Matamoro-Vidal, A., Y. Huang, I. Salazar-Ciudad, O. Shimmi, and D. Houle. 2018. Quantitative morphological variation in the developing Drosophila wing. G3 8:2399–2409.

McGuigan, K., J. D. Aguirre, and M. W. Blows. 2015. Simultaneous estimation of additive and mutational genetic variance in an outbred population of *Drosophila serrata*. Genetics 201:1239–1251.

McGuigan, K., L. Rowe, and M. W. Blows. 2011. Pleiotropy, apparent stabilizing selection and uncovering fitness optima. Trends Ecol. Evol. 26:22–29.

Menezes, B. F., F. M. Vigoder, A. A. Peixoto, J. Varaldi, and B. C. Bitner-Mathé. 2013. The influence of male wing shape on mating success in *Drosophila melanogaster*. Animal Behav. 85:1217–1223.

Meyer, K. 2007. WOMBAT – A tool for mixed model analyses in quantitative genetics by REML, *J.* Zhejiang Uni. SCIENCE B 8:815–821.

Meyer, K. and D. Houle. 2013. Sampling based approximation of confidence intervals for functions of genetic covariance matrices. Proc. Assoc. Advmt. Anim. Breed. Genet. 20:523–526

Mezey, J. G., and D. Houle. 2005. The dimensionality of genetic variation for wing shape in *Drosophila melanogaster*. Evolution 59:1027–1038.

Morrissey, M. B. 2016. Meta-analysis of magnitudes, differences and variation in evolutionary parameters. J. Evol. Biol. 29:1882–1904.

Pennell, T. M., F. J. H. de Haas, E. H. Morrow, and G. S. van Doorn. 2016. Contrasting effects of intralocus sexual conflict on sexually antagonistic coevolution. Proc. Natl. Acad. Sci. 113:E978–E986.

Pélabon, C., T. F. Hansen, A. J. R. Carter, and D. Houle. 2010. Evolution of variation and variability under fluctuating, stabilizing, and disruptive selection. Evolution 64:1912–1925.

Poissant, J., A. J. Wilson, and D. W. Coltman. 2009. Sex-specific genetic variance and the evolution of sexual dimorphism: a systematic review of cross-sex genetic correlations. Evolution 64:97–107.

Punzalan, D., and L. Rowe. 2015. Evolution of sexual dimorphism in phenotypic covariance structure in *Phymata*. Evolution 69:1597–1609.

R Core Team. 2019. R: A language and environment for statistical computing. R Foundation for Statistical Computing, Vienna, Austria. Available at https://www.R-project.org/.

Reddiex, A. J., Gosden, T. P., Bonduriansky, R., & Chenoweth, S. F. 2013. Sex-specific fitness consequences of nutrient intake and the evolvability of diet preferences. Am. Nat. 182: 91–102

Schluter, D. 1996. Adaptive radiation along genetic lines of least resistance. Evolution 50:1766–1774.

Sharp, N. P., and A. F. Agrawal. 2012. Male-biased fitness effects of spontaneous mutations in *Drosophila melanogaster*. Evolution 67:1189–1195.

Steven, J. C., L. F. Delph, and E. D. Brodie. 2007. Sexual dimorphism in the quantitative-genetic architecture of floral, leaf, and allocation traits in *Silene latifolia*. Evolution 61:42–57.

Sztepanacz, J. L., and M. W. Blows. 2017. Accounting for sampling error in genetic eigenvalues using random matrix theory. Genetics 206:1271–1284.

———. 2015. Dominance genetic variance for traits under directional selection in *Drosophila serrata*. Genetics 200:371–384.

Sztepanacz, J. L., K. McGuigan, and M. W. Blows. 2017. Heritable micro-environmental variance covaries with fitness in an outbred population of *Drosophila serrata*. Genetics 206:2185–2198.

Taylor, C. E., and V. Kekic. 1988. Sexual selection in a natural population of *Drosophila melanogaster*. Evolution 42:197–199.

Walling, C. A., M. B. Morrissey, K. Foerster, T. H. Clutton-Brock, J. M. Pemberton, and L. E. B. Kruuk. 2014. A multivariate analysis of genetic constraints to life history evolution in a wild population of red deer. Genetics 198:1735–1749.

Walsh, B., & Lynch, M. 2018. Evolution and selection of quantitative traits. Oxford Univ. Press, Oxford, U.K.

Walsh, B., and M. W. Blows. 2009. Abundant genetic variation + strong selection = multivariate genetic constraints: a geometric view of adaptation. Annu. Rev. Ecol. Evol. Syst. 40:41–59.

Weber, K. E. 1990. Increased selection response in larger populations. I. Selection for wing-tip height in *Drosophila melanogaster* at three population sizes. Genetics 125:579–584.

White, S. J., T. M. Houslay, and A. J. Wilson. 2018. Evolutionary genetics of personality in the *Trinidadian guppy* II: sexual dimorphism and genotype-by-sex interactions. Heredity 122:15–28.

Wolak, M. E., P. Arcese, L. F. Keller, P. Nietlisbach, and J. M. Reid. 2018. Sex-specific additive genetic variances and correlations for fitness in a song sparrow (*Melospiza melodia*) population subject to natural immigration and inbreeding. Evolution 72:2057–2075.

Wright, A. E., M. Fumagalli, C. R. Cooney, N. I. Bloch, F. G. Vieira, S. D. Buechel, N. Kolm, and J. E. Mank. 2018. Male-biased gene expression resolves sexual conflict through the evolution of sex-specific genetic architecture. Evol. Lett. 2:52–61.

Wyman, M. J., and L. Rowe. 2014. Male bias in distributions of additive genetic, residual, and phenotypic variances of shared traits. Am. Nat. 184:326–337.

Wyman, M. J., J. R. Stinchcombe, and L. Rowe. 2013. A multivariate view of the evolution of sexual dimorphism. J. Evol. Biol. 26:2070–2080.

Associate Editor: J. McGlothlin
Handling Editor: Mohamed A. F. Noor

Supporting Information

Additional supporting information may be found online in the Supporting Information section at the end of the article.

Supplementary Table 1. The first 20 principal components of the phenotypic covariance matrix of 24 x-y-landmark coordinates. Prop. of variance denotes the proportion of total phenotypic variance accounted for by each principal component.

Supplementary Table 2. The unit length vectors of: within-species sexual dimorphism, maximum among species variation in sexual dimorphism, and minimum among species variation in sexual dimorphism.

Supplementary Table 3. G_{mf} of 24 x-y-landmark coordinates for each sex that was obtained by back-transforming the 40-dimensional G_{mf} of principal component traits to the original coordinates.

Supplementary Table 4. G_{mf} of 20 principal component traits in each sex.